Chapter 2
Literature Review

We address a complex airspace planning and collaborative decision making model (APCDM) in this dissertation. The problem requires evaluating several aircraft flight plans, each of which are proposed along with several alternatives. These flights must be scheduled in such a way that we maximize the use of a limited airspace without compromising established safety requirements, while accounting for restrictions induced by Special Use Airspaces (SUA) and weather-related airspace closures. The selected flights must be distributed in time and space sufficiently so that the resulting traffic density does not exceed air traffic controllers' capacity to safety monitor and deconflict. Since the demand for flights can approach or exceed NAS capacity, particularly during peak periods, some aircraft flights must be delayed or be assigned sub-optimal flight trajectories. The proposed model will distribute the resulting fuel, delay, and other such costs between the airline participants in an equitable manner.

Accordingly, in Section 2.1 we discuss several air traffic management issues, and in Section 2.2 we outline techniques used to mitigate such issues as airspace congestion and flight delays. In Section 2.3 we review a success example from the FAA-sponsored Collaborative Decision Making initiative, and we provide in Section 2.4 the theoretical framework subsequently used in Chapter 5 to implement a CDM-based equity approach to the ASP. We examine the impact to the NAS from weather-related airspace closures as well as from space launch activities in Section 2.5. We conclude our literature review with an overview of previous models that have laid the groundwork for the model proposed in this dissertation.

2.1. National Airspace Traffic Density Issues

The Federal Aviation Administration (FAA) is in the midst of a 10-year sustained effort to modernize the National Airspace (NAS) to increase capacity by 30 percent. Currently, air traffic density is such that a single severe weather system can cause takeoff and landing delays that cascade throughout the entire NAS. During 2000, the top 55 airports conducted more than 20.8 million such operations, with 425,000 of them subject to delays [13].

Willemain [52] developed a simulation model to explore the impact of various parameters on blind collision risk in en route sectors. He concluded that the most important factors contributing to collision risk are the timing and quantity of aircraft entering a sector. Hence, a strategic optimization approach to schedule aircraft flights will have the greatest effect to increase air traffic density without exceeding Air Traffic Control capacity. This conclusion provides a foundational framework for the APCDM model we develop in this dissertation.

2.1.1. Ground Delay Program

The FAA executes a Ground Delay Program (GDP) when inbound traffic to an airport is predicted to exceed the airport's capacity. GDP delays flights at their respective origins to reduce the arrival rate at the constrained airport. Weather conditions are the primary cause for reductions in an airport's capacity, but airport capacity may also be exceeded when shifting flight schedules cause a surge in inbound traffic. GDPs are used as a lower-cost, and safer, alternative than holding aircraft in a traffic pattern over the destination airport. Nonetheless, GDPs are costly to enact, particularly if they are used inefficiently. The Air Transport Association estimates that each minute of delay costs an airline $29 [10].

2.1.2. High Density Airports and Slot Lotteries

The High Density Traffic Airports Rule (HDR) was created in 1968 to address capacity constraints at the nation's five busiest airports. HDR was initially applied to the following airports: John F. Kennedy International Airport, LaGuardia Airport, O'Hare

International Airport, Ronald Reagan National Airport, and Newark International Airport. HDR restrictions for Newark were discontinued in the early 1970s.

HDR limits air traffic at an airport by rationing allowable takeoffs and landings via a slot assignment system. A specified number of slots are created for each hourly or half-hourly time increment, and these slots are allocated by lottery to airlines that use the airport. Slot assignments effectively restrict the traffic demand in and around the airport to be within normal operating limits. Ownership of a slot gives an airline the exclusive right for one of its aircraft to land at or depart from the airport during the specified time interval. Slot lotteries are designed to ensure an equitable distribution of landing and takeoff rights among the various airlines.

In April 2000, the US Congress passed the “Wendall H. Ford Aviation Investment and Reform Act of the 21st Century” (AIR-21). This legislation modified Title 49, the United States Code (USC) from which the FAA derives its authority to regulate and control the NAS. AIR-21 provided slot restriction exemptions at small-hub and non-hub airports for new entrant airlines to establish service and thereby enhance market competition.

The impact of AIR-21 was swift and particularly burdensome to LaGuardia Airport. LaGuardia’s prime location, just seven miles from midtown Manhattan, made the airport very attractive to airlines establishing new services. In the six months following the legislation’s passage, more than 300 exemptions were granted resulting in severe congestion and air traffic delays. During September 2000, more than 9000 delays were reported at LaGuardia, an increase of 238% from six months earlier, that accounted for nearly one fourth of delays in the NAS [53]. Delays originating at LaGuardia propagated, causing additional traffic bottlenecks throughout the country.

In December 2000, the FAA acted to reduce the congestion at LaGuardia. Operations were limited to 75 per hour effective January 31, 2001. Given the existing slot assignments, the new restrictions limited the number of allowable AIR-21 exemptions to 159, versus the 300+ already in use. The FAA acknowledged that the dramatic reduction of slot exemptions would require termination of service to many small communities and would severely impair the ability of new entrants to compete with established carriers. However, the FAA also recognized that the airspace surrounding

LaGuardia is finite and capable of only limited short-term growth. On December 4, 2000, the FAA conducted a slot lottery to allocate the 159 slot exemptions.

Slot lottery procedures are published in Title 14, the Code of Federal Regulations (CFR). First, qualifying carriers are entered in a random drawing to determine the selection order. In the first round, new entrant and limited incumbent carriers make slot selections four at a time (two for arrivals and two for departures). Carriers serving small-hub and non-hub airports make two selections at a time during the second and third rounds. All carriers participate in the fourth and subsequent rounds until all available slots are allocated.

The auction of slot exemption operations was intended as a stopgap measure with the allocations effective only through September 15, 2001. During this period, the FAA was tasked to develop a more permanent solution to the congestion at LaGuardia. However, such a solution has so far been elusive and the FAA has extended the slot exemption restrictions and the current allocation through October 26, 2002 [21]. In addition, a supplemental auction was held in August 2001 to allocate some 21 residual slots.

As an aside, we noted that Midway Airlines was awarded 15 slots at the December 2000 auction. The airline filed for bankruptcy protection in early 2001, but was able to continue operations. However, in the aftermath of the terrorist attacks against the United States on September 11, 2001, Midway terminated operations permanently in anticipation of insufficient passenger demand to sustain the firm in the mid- to long-term future. Hence, Midway's 15 slots at LaGuardia Airport are currently unused and could be reallocated to other airlines, once full-capacity operations resume.

2.1.3. Hubbing

Airline route networks and schedules use a concept called *hubbing*, whereby origin-destination flights are routed through connecting terminals as opposed to adopting non-stop direct routes. Hubbing allows aircraft to be filled nearer to capacity than would be possible via direct routing. For example, passengers from different origins, but with the same fixed destination, can depart airports and subsequently connect to a common flight at a hub that will take them to their final destination.

Hubbing is an efficient scheduling technique, but it is extremely sensitive to schedule disruptions such as those caused by inclement weather.

To effectively utilize the capacity of an aircraft departing a hub, the various incoming flights (from which passengers will transfer to the outgoing flight) are scheduled to arrive at the hub within a short time interval, a process called *banking*. When airport capacity is constrained or when flights are delayed or cancelled, the airline must decide whether to delay inbound flights ("spreading the bank") and whether any flights must be separated from their respective bank. Separating a flight is a relatively costly decision, as a late incoming flight may cause passengers to miss connecting flights and generate a cascading effect on downstream flights.

Milner (1995) authored the first decision-support model to handle schedule disruptions that included consideration of hubbing. Later, Carlson [8] made a number of practical improvements to Milner's formulation. First, he included flights that were independent, that is, not part of a bank. Next, the model was designed to prohibit certain flights from being separated from their respective bank. Finally, he incorporated delay costs, a consideration that was previously absent.

Carlson [8] also presented multiple alternative formulations. The first was essentially that of Milner, with step-function variables, while the second formulation replaced these with the more traditional binary form. In his third model, the set of cancellation variables was removed. This approach is interesting, as it allows the problem to be viewed from a different angle. The first two models begin with flights arriving as scheduled, and then the solution algorithm cancels or delays flights as necessary to achieve a prescribed solution. The third model algorithm begins with all flights as cancelled and then assigns flights, subject to the capacity constraints, as close as possible to the scheduled arrival times. This approach reveals that we may be able to find more efficient solution methodologies by changing the "paradigm" of our problem formulation.

2.1.4. International Terrorism

Any discussion of the NAS would unfortunately be incomplete without mention of international terrorism following the events of September 11, 2001. Four commercial

airliners were hijacked with three being purposefully collided with the World Trade Center towers and the Pentagon. This unprecedented act of terrorism sent shockwaves throughout the United States and particularly through the airline industry.

Following the terrorist attacks, consumer confidence in flight safety plummeted. Travel during the Thanksgiving 2001 holidays on the major airlines suffered a 25 to 30 percent [5] decline relative to the previous year, despite considerable incentives offered by the airlines in the form of reduced fares.

Increased security measures were implemented in the months following the attacks. In February 2002, the U.S. Government implemented a 100 percent Positive Passenger Bag Match (PPBM) policy, wherein each piece of checked baggage must be positively matched against a confirmed boarded passenger. In addition, the federal government assumed full responsibility for airport security, with federal workers assuming duties previously held by private contractors.

While the increased security may well enhance passenger safety, there is a significant cost to passenger convenience. There is, for example, ample anecdotal evidence of the indignities suffered by passengers at security checkpoints. Moreover, to have sufficient time to proceed through the various security checks, passengers are now required to arrive at airports more than two hours in advance of the scheduled flight take-off time. As a result, much of the time advantage previously gained by flying rather than by taking ground transportation is forfeited, particularly for shorter regional flights.

There exists minimal precedence to gauge the long-term impact of this event and the ensuing policies on air travel. Barnett [5] observes that the three downed airliners resulted in more deaths (passengers and ground casualties) than all previous domestic crashes combined. For now, air traffic density across the NAS is significantly reduced. However, while the recovery timeline [4], depicted in Figure 2-1, is uncertain, it is likely that customer demand will, within the next few years, return to normal levels, and then resume its historical growth pattern.

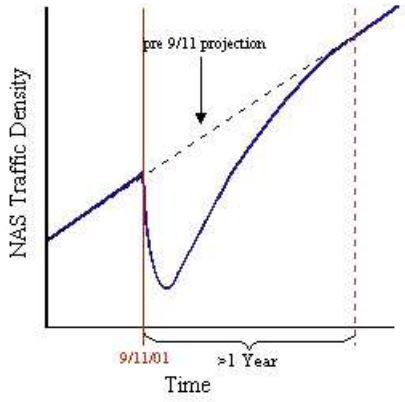

Figure 2-1: Attack Recovery Timeline

2.2. Collision Detection

2.2.1. Separation Standards

Reich [43] defined a set of necessary considerations for safe, practical, and least-cost aircraft separation standards. Aircraft separation standards are used to safeguard against the uncertainties in aircraft position in the along-track, cross-track, and vertical axes. Reich identified an economic optimum separation standard as one that minimizes the costs to airlines from route deviations required by the standards and the costs of collisions. Today, FAA standards require that aircraft maintain a 5 nautical mile horizontal separation and a vertical separation of 2,000 feet for aircraft above 29,000 feet and 1,000 feet below this altitude [41].

Reich modeled the separation restrictions by using a geometric box, called a proximity shell, aligned with the aircraft velocity vector, and described about the instantaneous position of each *focal* aircraft. The air traffic controller's task is then to ensure that no *intruder* aircraft's position ever lies within this box. The box is defined such that when other aircraft remain outside the box, the risk of collision is negligible. Collision risk is defined as the expected number of collisions in a given interval of time. Reich's analysis requires two probability distributions to describe the variations about the intended trajectory: the error magnitudes and the rates of change of error magnitudes (i.e. wavelengths and oscillations about intended position). Observe that we can simplify the calculations by treating the focal aircraft as a deterministic point and then assigning the aggregate uncertainties and proximity shells to the intruder aircraft.

Reich [43] stresses the importance of the geometry of intrusions into the proximity shell of the focal aircraft. That is, the risk of collision and the period the aircraft are exposed to this risk is a function of the relative aircraft vectors. For example, a head-on encounter differs greatly from aircraft near-paralleling each other.

2.2.2. Miles-in-trail Spacing

Air traffic controllers use miles-in-trail (MIT) spacing restrictions between aircraft to distribute incoming traffic at busy terminal destinations. MIT spacing may also be used to alleviate airspace congestion. The re-routings required to implement MIT spacing affect an estimated 540,000 flights annually with a fuel penalty cost of nearly $45 million [23].

There is an inherent ATC workload imposed to establish MIT streams. These streams in turn concentrate air traffic in specific sectors with a corresponding further increase in workload. Furthermore, an optimized set of aircraft flight plans may still be subject to re-routing to establish traffic streams that enforce MIT spacing. Hence we might desire an enhanced solution that also minimizes the need for MIT spacing.

One approach is to increase the length (in the in-trail axis) of the proximity shell around each focal aircraft for the purpose of an optimization model. However, this will prove to be overly restrictive. For example, the increased shell size would apply regardless of the flight's destination, which may not be appropriate for destinations having a low traffic density. More importantly, the enlarged shells would generate false conflicts, causing the model to reject acceptable flight plans.

A superior approach is to assess a terminal area workload penalty similar to that used for en route sector workloads and then to accordingly impose a penalty for excessive terminal area densities.

2.2.3. Conflict Prediction

Paielli and Erzberger [41] noted that during flight, the prediction of aircraft trajectories is not an exact science. For example, wind modeling is still quite imprecise, aircraft navigation and control equipment are not error-free, and finally, there's the human element—the pilot. The pilot makes inexact course corrections based on

instrumentation and his or her own perception, which yields additional variance from the planned or predicted course.

We can examine error prediction in four dimensions: cross-track (latitudinal), along-track (longitudinal), vertical, and time. Paielli and Erzberger [41] found that errors in the cross-track axis were relatively constant at 0.5 to 1.0 nautical miles (nm) in a 30-minute period, as they are routinely corrected by the pilot or the aircraft's flight management system. The along-track errors are significantly more variable, being created primarily by headwinds and tailwinds, which are not well predicted nor easily corrected for during flight. The accumulated errors over time were found to grow linearly at a rate of 0.25 nm per minute. While vertical errors were generally found to be more prevalent during climb, descent, and turning, the errors occurring in level flight were typically confined to less than 400 feet. Due to the computational difficulties of estimating the vertical errors, Paielli and Erzberger [41] confined their study to level flights, noting that, in this case, the vertical conflict probability, for practical purposes, was zero for predicted separations of more than 2,600 feet and unity when less than 1,400 feet.

Observe that the passage of time increases uncertainly with respect to an aircraft trajectory. That is, the longer in advance a trajectory is to be predicted the more likely a larger prediction error occurs. Paielli and Erzberger [41] empirically showed this through their study at the Fort Worth Air Route Traffic Control Center (ARTCC). Moreover, they demonstrated that the flight path prediction errors in the horizontal plane could be approximated by a Normal distribution. An analytical solution was then derived to predict conflicts between aircraft pairs in the horizontal plane.

Paielli and Erzberger [41] astutely observed that the decision for when to initiate a conflict resolution maneuver (where at least one of the aircraft changes trajectory to avoid the potential conflict) involves a tradeoff between an efficient maneuver versus the certainty that a conflict will occur. A maneuver initiated too early may have been unnecessary because the conflict prediction becomes increasingly coarse the further in advance it is calculated. However, waiting until the conflict is near certain would require a more severe maneuver resulting in wastage of fuel and lost time.

Paielli and Erzberger [42] subsequently extended their model to include non-level flights. While their methodology did not produce an exact analytical solution, they developed a close approximation that was found to yield satisfactory results. In their discussion, they listed some "caveats" regarding the limitations and assumptions required for the updated model. The approach assumes constant velocities for both aircraft during the time of predicted conflict, which may not always be the case. In cases where the two aircraft have small relative velocities, predictions are susceptible to wind-errors. Lastly, ARTCC computers process aircraft altitudes that are within 200 feet of cleared altitudes as being at the cleared altitude. For a pair of aircraft, this can yield conflict predictions based on relative altitudes that are as much as 400 feet in error.

Bakker, Kremer, and Blom [3] experimented with both geometric and probabilistic approaches to conflict prediction. In contrast to previous work, they examined trajectory errors in three dimensions simultaneously, rather than assigning independent error distributions for each axis. They concluded, as previous researchers have, that a probabilistic approach is a necessary part of modeling collision prediction.

2.2.4. Center-Tracon Automation System

Conflict prediction algorithms are run as a routine, called a "Conflict Probe," and are incorporated into the software of the Center-TRACON Automation System (CTAS) [16]. CTAS is not only used to predict conflicts, but is also used to calculate the flight corrections necessary to bring the probability of a separation violation below a programmed threshold. CTAS is designed to be a real-time tool to aid air traffic management and has been installed for testing at two ARTCCs for testing and validation [42].

McNally, Bach, and Chan [28] reported the results of field testing at the Denver ARTCC, where a Conflict Prediction and Trial Planning (CPTP) tool was incorporated into the CTAS. The enhanced tool includes an improved conflict prediction algorithm and uses conflict probability estimation. Conflict predictions are updated every 6 seconds.

The user interface allows real-time "what-if" trials for flight plans to resolve conflicts. If the proposed plan resolves the conflict and creates no new conflicts, the air

traffic controller can accept the plan and issue a clearance to the affected aircraft. Controllers noted that this capability was especially useful. The trial-planning tool allowed the controller to look ahead on a more strategic basis, verify a conflict-free clearance, and issue this clearance to the pilots prior to the conflict becoming a tactical issue.

Using the CPTP, controllers were able to issue a direct clearance more than twice as often versus issuing a vectoring clearance to resolve a conflict. The vector approach requires a second clearance to return to a post-conflict flight trajectory, while the direct clearance, having been verified as conflict-free, requires no follow-up action. In addition, direct-route conflict resolution could potentially provide a 12.1 nm flight length savings per aircraft. During the Denver experiment, an actual average savings of 3.4 nm was realized [28]. The difference was attributed to compliance with real-world constraints plus navigation and track errors. Nevertheless, the savings is substantial.

2.2.5. Direct-to Tools

Erzberger, McNally & Foster [15] developed a Direct-to Tool for use by en route Air Traffic Controllers to identify real-time direct-to routings for aircraft. A direct-to routing specifies a straight-line trajectory from the aircraft's current location to a navigation fix or waypoint. This routing may bypass intermediate waypoints laid out in the original flight plan. Depending on the spatial wind field in the region, the direct-to route may decrease or increase the time to fly to the destination. The authors noted that flight time, as opposed to flight distance, was the appropriate measure of efficiency.

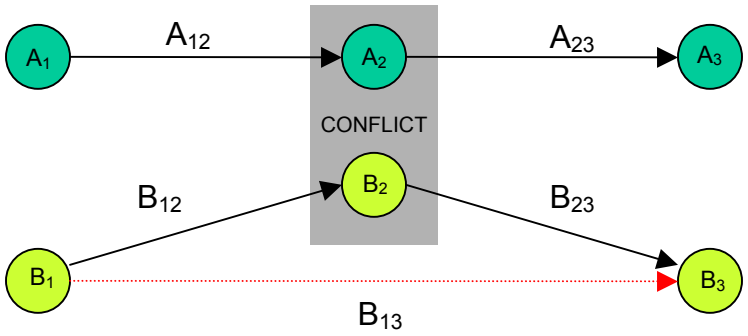

Figure 2-2: Direct-to Routing Example

Consider the scenario diagrammed in Figure 2-2. Each flight plan A and B is shown having three waypoints. The second waypoint of each respective aircraft is such that there is a conflict between these two flight plans. The conflict can be avoided by constructing a new flight plan that includes a direct-to routing for aircraft B from node B_1 to B_3 via segment B_{13}. Depending on a number of factors, the new flight plan may not necessarily be as efficient as the original one, but is feasible in that there is no longer a conflict between the pair of flight plans A and B. To implement this methodology, a model would need to examine segments where conflicts occur, identify the waypoints that are adjacent to the spatial conflict region, generate a surrogate flight plan that omits the conflicting segment by using a direct routing between the adjacent waypoints, and finally evaluate the new flight plan for feasibility, desirability, and optimality.

2.3. Collaborative Decision Making (CDM)

CDM is essentially a business practice that advocates decentralized cooperative decision making between the various participants in a common endeavor. CDM takes advantage of many of the "Total Quality Management" precepts [50] that were advanced and popularized by W. Edwards Deming in Japan during the 1970s and 1980s, and later in the United States during the early 1990s. Revolutionary improvements in air traffic control are needed due to a continuing 1.5 - 3 percent annual growth rate in the number of flights in the NAS. The advent of the "Free-Flight" paradigm further complicates air traffic control in an increasingly crowded airspace [48]. The FAA is sponsoring a comprehensive CDM effort to improve air traffic management, increase capacity, and to reduce costs.

2.3.1. Ground Delay Program Enhancement

The implementation of the Ground Delay Program Enhancement (GDPE), the first major thrust of CDM [29], is an impressive example of CDM success. The GDPE effort implements three central tenets of CDM. First, GDPE creates a common situational awareness between the FAA and the 24 currently participating airlines [18]. Next, a distributed planning environment is designed where the roles and

responsibilities of the players are agreed upon and well-understood, limited resources are rationed equitably, and all participants have a voice in the decision process. Finally, a performance measurement and feedback process is supported to facilitate system improvements.

Chang et al. [10] reported a number of difficulties with previous GDP processes. Most importantly, command centers had sparse information concerning updates to flight schedules made by airlines, while airlines did not have information concerning changes to airport arrival demands and capacities. The GDPE team developed databases, communications architecture, and update mechanisms to allow real-time information sharing between all concerned parties. For example, users now have access to the Enhanced Traffic Management System (ETMS), and can obtain complete FAA information for updating their portion of the overall data through a standardized interface.

GDP procedures were modified to eliminate disincentives for airlines to report flight schedule changes, particularly delays and cancellations. Previously, GDP delayed flights based on arrival time. Hence if an airline reported a delay, GDP would delay the flight even further, called a “double penalty.” Today, GDP flight delays are instead based on the originally scheduled flight time. Prior to the GDPE effort, airlines would lose the respective arrival slot upon reporting a flight cancellation, which prevented the airline from substituting a new flight for the cancelled one. Today, when an airline cancels a flight, it has first priority to utilize the freed arrival slot by utilizing a *compression algorithm*.

When a slot is opened as the result of a cancellation or delay, the compression algorithm looks first for another flight belonging to the same carrier to move into this slot. The carrier uses its own prioritization scheme to determine availability. If the carrier does not have an available flight, the algorithm selects the next available flight, giving preferences to carriers participating in CDM. Chang et al. [10] report that this algorithm is a “win-win” situation for the carriers, in that compression reduces delays while, at worst, preserving the status quo for a given carrier. The implementation of compression concepts has made it advantageous for the airlines to report schedule

changes as they occur. This provides FAA command centers the ability to plan GDP decisions using substantially more accurate information.

The result is a distributed decision structure, rather than a hierarchal one, that has dramatically reduced airline delay costs. For example, over a two-year period, the compression algorithm alone reduced delays by 4.5 million minutes versus the previous GDP procedures [10].

2.3.2. NAS Performance Measurements

Hansen et al. [24] used a statistical cost estimation methodology to investigate the relationship between improvements in NAS performance and airline costs. They began with seven commonly accepted performance metrics: average arrival delay, average departure delay, average >15 minute arrival delay, arrival delay variance, departure delay variance, unreliability (percentage of flights arriving more than 15 minutes late), and the cancellation rate. These metrics were determined to be highly inter-correlated, hence, the authors used several techniques to generate alternative two-factor (delay and irregularity) and three-factor (delay, variability, and disruption) representations, where these factors were reasonably independent. Both cost models were compared against historical NAS quarterly performance data to statistically estimate an airline cost function. They observed that changes in NAS performance did not appreciably affect flight delays. In contrast, the schedule disruption metric emerged as the most significant measure of NAS efficiency. Of the original seven factors, the flight cancellation rate correlated best with this metric. One conclusion drawn from this is that an airline operations strategy that avoids flight cancellations, even when delayed significantly, might be more efficient than strategies that seek to minimize average delays. Hanson et al. recommend making NAS investments that improve the robustness of NAS operations (i.e., reliability and predictability), rather than those that yield incremental improvements in delay times.

2.4. Utility Theory

Utility theory owes much of its origin as a means to explain economic behavior. There is a great deal of literature dating back to the 18th and 19th centuries, with

particular growth in utility theory during the last half-century. Contributions have emerged from the fields of economics, statistics, mathematics, psychology, and management science [20].

Utility models are broadly used to explain consumer behavior and values in a free-market economy. The classical supply and demand curves are examples. In such a model, a utility function is drawn in the (x, y) space, where x is the consumption of a particular commodity, and y is a second commodity against which the first is traded. The y-axis can alternatively depict the unit price of x. The function hence drawn is called an indifference curve. The individual derives equal benefit (or utility) from any (x, y) pair along the curve. A series of parallel curves can be drawn to show different levels of utility. Figure 2-3 displays examples of common utility function forms used in economics [34]. Note that intersecting curves would indicate inconsistent preferences.

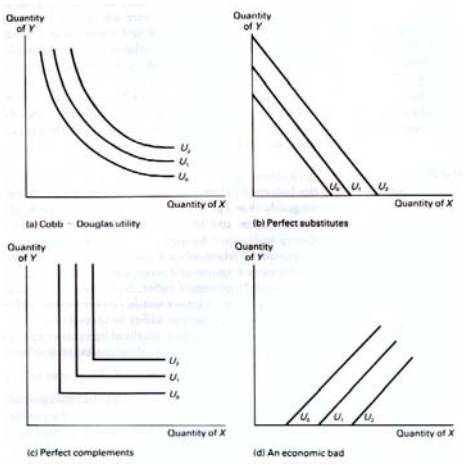

Figure 2-3: Common Utility Function Forms

Particularly during the latter half of the 20th century, utility theory has been used, with increasing sophistication, to model the perceived value of decision alternatives. Using mathematical models to explain human behavior is full of challenges, but given an appropriate set of assumptions, utility models are quite useful to both *describe* and *prescribe* decisions [25].

We use utility theory concepts to derive mathematical functions to describe a preference structure over a set of alternatives. Clemen [11] has provided a set of

axioms, presented in Table 2-1, from which it can be shown in general that people are able to rank order all possible situations from the most desirable to the least. Utility functions can also be used to mathematically express an intensity of preference between two or more alternatives.

Completeness: If A and B are any two alternatives, a decision maker (DM) can specify exactly one of the following three possibilities, and the ordering is transitive: a. "A is preferred to B" (A > B) b. "B is preferred to A" (B > A) c. "DM is indifferent between A and B" (A ~ B)
Reduction of Compound Uncertain Events: A DM is indifferent between a compound uncertain event and a simple uncertain event as determined by reduction using standard probability manipulation.
Continuity: A DM is indifferent between an outcome A and some uncertain event involving only two basic outcomes A_1 and A_2, where $A_1 > A > A_2$. In other words, for each event, a reference gamble can be formulated with probability p, for which the DM will be indifferent between the reference gamble and A.
Substitutability: A DM is indifferent between any original uncertain event that includes A and one formed by substituting for A an uncertain event that is deemed equivalent to A.
Monotonicity: Given two reference gambles with the same possible outcomes, a DM prefers the one with higher probabilities of winning the preferred outcome.
Invariance: All that is needed to determine a DM's preferences among uncertain events are the payoffs for outcomes and the associated probabilities.
Boundedness: No outcomes are considered infinitely good or infinitely bad.

Table 2-1: Utility Theory Axioms

Decision makers typically exhibit risk-prone, risk-averse, or risk-neutral behavior. Figure 2-4 shows the general shape of utility curves for each type of risk behavior.

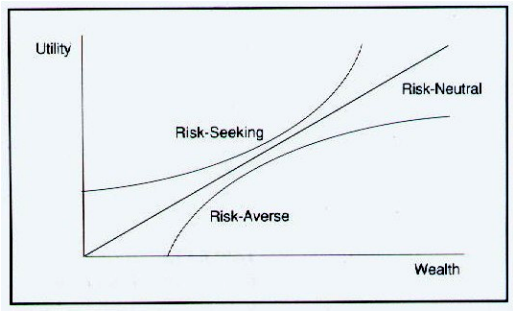

Figure 2-4: Risk Behavior

We can estimate a univariate utility function by asking the DM a series of *lottery (reference gamble) questions* and use the answers to determine certainty equivalents. A lottery question is constructed as depicted in Figure 2-5. A person is given the choice between a sure outcome C and a lottery between outcomes A and B such that the probability that A occurs is p, and the probability that B occurs is $(1-p)$, where $A \succ C \succ B$ (where "$\succ$" denotes "is preferred to").

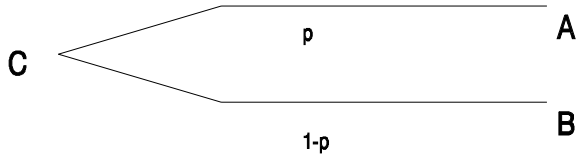

Figure 2-5: Reference Gamble

Fractile and bracketing methods, which use this approach, can be quite cumbersome in real-world applications. For example, there are at least four methodologies used to set up the series of reference lottery questions required to elicit DM preferences. A large volume of research has been dedicated to showing that the methodology chosen can bias an individual's responses. Furthermore, when we compare the utility functions constructed using different response methods, we often find contradictory preferences [20].

Kirkwood [27] proves that if the DM exhibits a constant risk tolerance across the range of the attribute under consideration, then the resulting utility function will take either a linear or exponential form. If preferences are monotonically increasing (more of x is preferred) over $x_{\min} \le x \le x_{\max}$, then,

$$U(x) = \begin{cases} \dfrac{\exp\left[\dfrac{-(x - x_{\min})}{\rho}\right] - 1}{\exp\left[\dfrac{-(x_{\max} - x_{\min})}{\rho}\right] - 1} & \rho \neq \infty \\ \dfrac{x - x_{\min}}{x_{\max} - x_{\min}} & \text{otherwise} \end{cases}, \tag{2.1}$$

and if preferences are monotonically decreasing (less of x is preferred) over $x_{\min} \le x \le x_{\max}$, then,

$$U(x) = \begin{cases} \dfrac{\exp\left[\dfrac{-(x_{\max} - x)}{\rho}\right] - 1}{\exp\left[\dfrac{-(x_{\max} - x_{\min})}{\rho}\right] - 1} & \rho \neq \infty \\ \dfrac{x_{\max} - x}{x_{\max} - x_{\min}} & \text{otherwise} \end{cases}, \tag{2.2}$$

where ρ is called the *risk tolerance*. (Note that the second case, for both of (2.1) and (2.2), is simply the limiting value of the first case as $\rho \to \infty$.) After we elicit from the DM the value of x^* such that $U(x) = 0.5$, we can calculate ρ as the numerical solution to the equation,

$$0.5 = \frac{\exp\left[\dfrac{-(x^* - x_{\min})}{\rho}\right] - 1}{\exp\left[\dfrac{-(x_{\max} - x_{\min})}{\rho}\right] - 1} \quad \text{for} \quad x^* \neq \frac{x_{\max} + x_{\min}}{2}, \tag{2.3}$$

when $U(x)$ is a monotonically increasing utility function and

$$0.5 = \frac{\exp\left[\frac{-(x_{\max} - x^*)}{\rho}\right] - 1}{\exp\left[\frac{-(x_{\max} - x_{\min})}{\rho}\right] - 1} \quad \text{for} \quad x^* \neq \frac{x_{\max} + x_{\min}}{2}, \tag{2.4}$$

when $U(x)$ is a monotonically decreasing utility function. Observe that for both increasing and decreasing utility functions,

$$\rho = \infty \quad \text{when} \quad x^* = \frac{x_{\max} + x_{\min}}{2}, \tag{2.5}$$

and the resulting function is linear. Empirical results have shown this to be a very satisfactory method to estimate preferences [49].

Most decision problems are not based on a single criterion. There are often multiple, sometimes competing, objectives for which the DM wishes to maximize utility. We can use Multi-attribute Utility Theory (MAUT) techniques to aggregate individual utility functions into a single multi-criterion utility function. Construction of a multi-criterion utility function can be a complex task. Most importantly, the process requires that the attributes be independent of each other. Zeleny [54] outlines three necessary forms of independence as described in Table 2-2.

Preferential Independence: Concerned with ordinal preferences. A pair of attributes, X and Y, are preferentially independent of a third, Z, if the value trade-off between X and Y is not dependent upon the value of Z.
Utility Independence: Concerned with cardinal preferences. If lottery preferences of attribute X do not depend on the value of Y, then X is utility independent of Y. In general, X being utility independent of Y does not imply the reverse. When the reverse holds, X and Y are said to be mutually utility independent, a necessary condition for a multiplicative utility function.
Additive Independence: The strongest form of independence. Lottery preferences of X do not depend on changes in lotteries for Y. That is, uncertain outcomes for multiple attributes can be evaluated one attribute at a time. This is a necessary condition for an additive utility function that rarely holds in real situations.

Table 2-2: Utility Independence

The additive multi-criteria utility function takes the form,

$$U(x_1, x_2, ..., x_n) = w_1 \cdot U_1(x_1) + w_2 \cdot U_2(x_2) + ... + w_n \cdot U_n(x_n) \text{ where } \sum_i w_i = 1, \quad (2.6)$$

and where w_i is a calibrated weighting factor assigned to the i^{th} univariate utility function. This form is computationally convenient, but as we noted in Table 2-2, additive independence is difficult to justify for most decision problems.

Clemen [11] has offered an interesting insight for the criteria weights. If the weights of a set of criteria sum to less than unity, they are said to be substitutes for each other. Conversely, if they sum to more than unity, they are called compliments to each other. In both of these cases, the multiplicative form of the multi-attribute utility function is appropriately used, and is given by,

$$U(X) = \frac{\prod_i \left(\kappa w_i U_i(x_i) + 1\right) - 1}{\kappa}, \text{ where } \kappa \neq 0. \quad (2.7)$$

Observe that (2.7) includes nonlinear terms. The normalizing factor κ is calculated by setting each attribute to its maximum value to yield $U(X) = 1$ and then solving for κ. For example, when the multiplicative utility function is composed of two attributes, κ is given by,

$$\kappa = \frac{1 - w_1 - w_2}{w_1 w_2}. \quad (2.8)$$

2.5. Applications Background

2.5.1. Space Launches

Commercial space launch is a growth industry in the United States. There is a burgeoning demand for space-based technologies, including multimedia communications, navigation, meteorology, reconnaissance, scientific research, and environmental monitoring. Hence there is a pressing need for space transportation to provide routine access to space, particularly for earth-orbiting satellites.

Space access from the United States has historically been provided by launch sites owned by the federal government at the Kennedy Space Center and Cape Canaveral Air Force Station in Florida, and Vandenberg Air Force Base, California. Recently, commercial spaceports were established in Florida and California (adjacent to the federal sites) and in Alaska and Virginia. As of 2002, there are 12 additional commercial sites being proposed. The proliferation of space launch sites (many at inland versus coastal locations) and the corresponding increase in launch rates is expected to make a dramatic impact on the NAS.

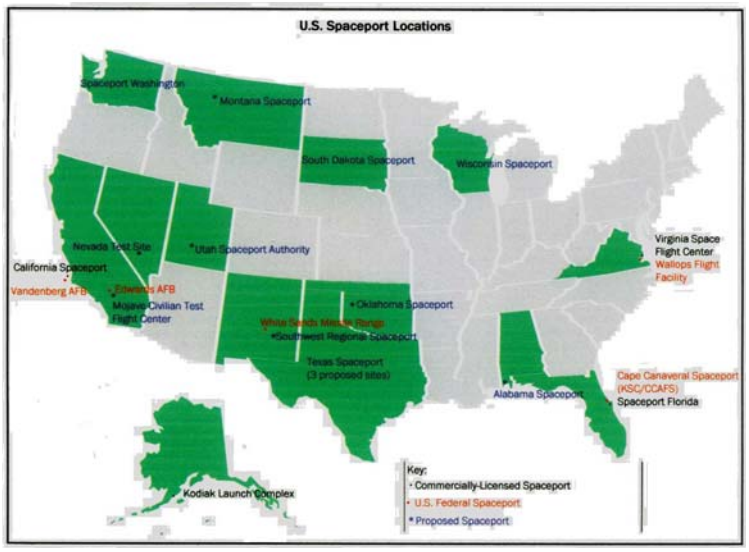

Figure 2-6: US Spaceport Locations [40]

Commercial space transportation is regulated by Title 49, United States Code, Section IX. This statute delegates responsibility for space launch activities to the Office of the Associate Administrator for Commercial Space Transportation (AST), which is a part of the FAA. AST publishes guidance for planning, licensing, and executing space launch activities. In addition, AST is beginning to develop guidance for future commercial re-entry operations.

One of AST's biggest long-term projects is to develop and refine an integrated Space and Air Traffic Management System [38]. AST has published a Concept of Operations (CONOPS) that describes future commercial space launch and re-entry operations, particularly as these vehicles traverse through the NAS.

The CONOPS defines two new airspace structures for the NAS that will replace the current SUAs. First, *Space Transition Corridors* (STCs) are dynamically reserved and released airspace regions that are designed to be more flexible than SUAs, and are to be used for space vehicles transitioning in and out of the NAS. Second, *Flexible Spaceways* will be defined in a manner similar to current jet routes. Also flexible by design, these will be used for activities such as transitions to airborne refueling and launch points [38].

The primary impact to the NAS from current space launch activities arises from SUAs. Large portions of the NAS are closed to air traffic to accommodate the launch and recovery of space vehicles as they transition through the NAS. During the mission-planning process, an *Overflight Exclusion Zone* is calculated based on the type of launch vehicle and the specific mission requirements.

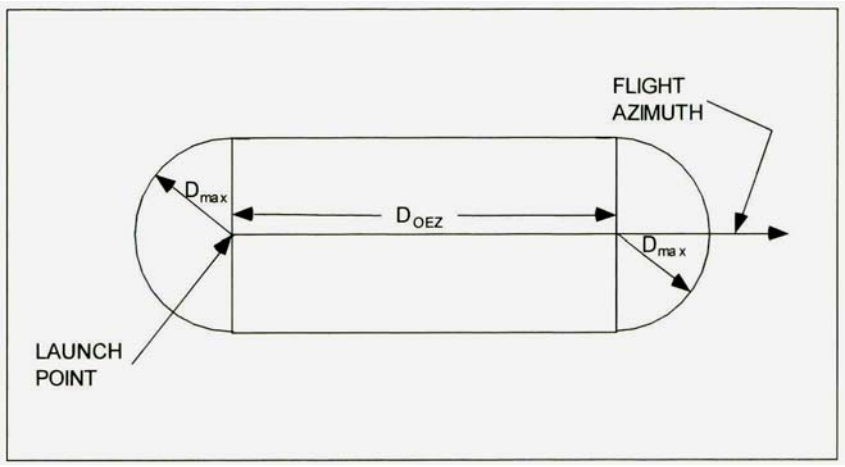

Figure 2-7: Overflight Exclusion Zone [39]

In Figure 2-7, $D_{\max}$ is defined as the *debris dispersion radius*, which is based on the size of the launch vehicle as measured by its lift capacity to low-earth orbit (100 nm). For example, the Delta II is classified as a medium class expendable launch vehicle (ELV) with $D_{\max}$ =1.53 nm. The variable D_{OEZ} is defined as the *overflight exclusion zone downrange distance* and is calculated using the mission-specific launch azimuth as well as the vehicle class. In the case of a Delta II ELV, D_{OEZ} will have a length of 3.47 nm. Overflight Exclusion Zones are initiated during the launch vehicle

terminal countdown prior to the opening of the launch window and are maintained until either the launch window closes, or following liftoff and transition through the NAS by the launch vehicle.

The CONOPS takes advantage of CDM concepts. For example, the CONOPS proposes information systems to enhance the "shared situational awareness" of the various NAS participants, to include advanced digital communications and enhanced real-time weather data. In addition, the NAS Wide Information System will provide a common exchange medium for static NAS information (maps, charts, NOTAMs, etc) as well as dynamic information such as STC status, space launch updates, weather forecasts, and air and space traffic monitoring [38].

2.5.2. Weather Systems

Weather phenomena provide a formidable challenge to air traffic control. In contrast to space launch SUAs, restricted airspace requirements arising from severe weather is exceptionally dynamic. Closed airspace regions are irregular shaped, move with respect to time, and change shape throughout a storm's cycle of development and subsequent dissipation. The duration and timing of severe weather is often difficult to predict. For example, thunderstorm cells can form unexpectedly and require airspace closures with little more than 30 minutes advance warning.

Nilim et al. [35] developed a dynamic trajectory-based routing strategy to investigate the impact on en route aircraft from probabilistic weather events. They compared a traditional routing strategy, which selects aircraft routes to avoid bad weather zones entirely, with a dynamic approach that risks costlier delays as a tradeoff against decreased expected weather-related delays. The stochastic dynamic programming algorithm's complexity is exponential with respect to the number of storm systems being considered.

2.5.3. Time-dependent Traffic Modeling

Vehicle streams can be represented in a three-dimensional diagram where the time domain is placed on the horizontal axis, the one-dimensional position is placed on the vertical axis, and the third axis shows the cumulative traffic density. With

appropriate transformations, these diagrams can be used to detect active bottlenecks in traffic flow. One such transformation is to use a reference vehicle's instantaneous position as the origin. This "moving time coordinate system" horizontally moves the cumulative count curves such that neighboring curves show vehicle delays and vehicle accumulations.

Cassidy [9] gives an interesting example showing how event location propagates through a free flowing traffic state as a shock. For example, the lead reference vehicle first travels at a nominal velocity for a period of time, slows and maintains a slower velocity for a period, then stops for a period, and finally accelerates to a new velocity for the final period. Subsequent vehicles, by model assumption, maintain a constant separation from the preceding vehicle. The result is that the transition points (slowing, stopping, accelerating) move backwards in time and position. For those that have observed a traffic jam, the model is especially revealing. Even after the cause of a traffic delay (e.g. an accident) is removed, traffic congestion persists and is located significantly upstream of the accident site. The peak congestion point continues to move upstream as it gradually dissipates. This is a non-intuitive result to the vehicle driver who is delayed at one location, and then sees evidence of the cause of the delay several miles downstream, where traffic is currently moving smoothly.

2.6. Relationships Between the Present and Previous Research

2.6.1. Airspace Occupancy Model

The Airspace Sector Occupancy Model (AOM) developed by Sherali et al. [48] is used to determine the occupancies by aircraft in the modules and sectors that comprise the NAS. The model examines a given set of flight plans and mathematically describes their flight trajectories over a defined region of airspace to determine sector crossings and occupancies as a function of time. This model is used to calculate information that is subsequently used in the Aircraft Encounter Model (AEM).

The AOM begins with a pre-processing routine to create a mathematical representation of the NAS. The entire airspace over the United States is divided into twenty-one centers, each regulated by an ARTCC. Each of these centers is divided into sectors. Sectors are well-defined airspace regions specified by the FAA for regulating

air traffic, and are classified into three groups: low, high, and super-high, depending upon their floor and ceiling boundaries. Low sectors lie below 24,000 feet (flight level (FL) 240). High sectors extend between FL 240 and FL 350. The super-high sectors lie above FL 350.

Each sector is comprised of Fixed Point Airspace (FPA) units and each of these FPAs is composed of modules. A module is an airspace region having a generally non-convex polygonal cross-section, and is defined by its vertices and its floor and ceiling altitudes. Included with the set of vertices that are input to AOM are pseudo-vertices. A pseudo-vertex is defined as a vertex for some other module that is present on a vertical face of the given module, but is not an original defining vertex of its floor and ceiling. The points formed by the two dimensional projection of either vertical edges or pseudo-vertices of a module onto its floor or ceiling are called nodes, and are used to define the floor and ceiling geometry of a sector module. Modules are stacked one over another to form an FPA, and several such adjacent FPAs form a sector. Figure 2-8 depicts a pair of adjacent sector modules.

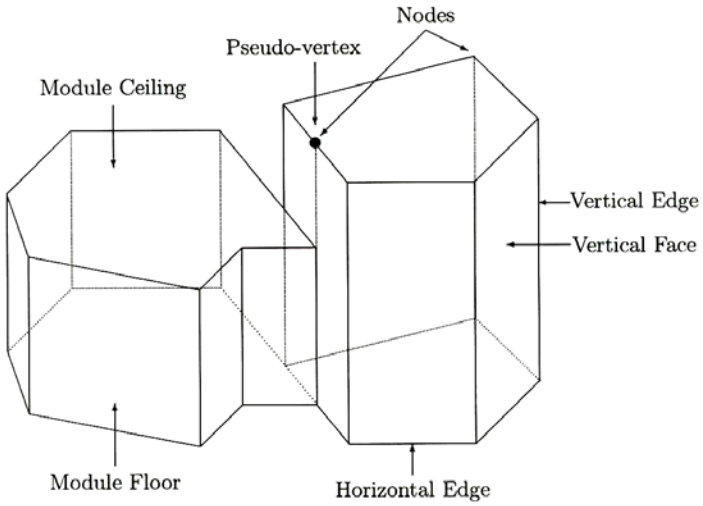

Figure 2-8: Sector Module Geometry [48]

Having created a mathematical representation of the NAS, AOM's pre-processing routine determines the set of adjacent sectors for each sector. Adjacency is defined such that for each sector s_i, sector s_j is adjacent if any module that is part of

sector s_j shares a common geometric face, edge, or vertex with a module that is part of sector s_i.

In the main routine, AOM considers each flight path that is comprised of linear discretized flight segments and having break-points represented in terms of the coordinates $wp_1, wp_2, ..., wp_n$ that it traverses. The i^{th} such linear segment trajectory is then defined as $wp_i + \lambda d$ for $0 \le \lambda \le 1$, where $d = wp_{i+1} - wp_i$. The algorithm looks for the point (and the associated time) where the trajectory intersects a vertex, edge, or face of the currently occupied module. At such a point, the algorithm determines whether the aircraft trajectory continues within the same module (sector) or transitions to an adjacent module (sector). Figure 2-9 shows an example where a flight transitions from some sector s to the adjacent sector $s+1$ as it traverses its i^{th} piecewise linear trajectory. Observe in the example that the AOM routine distinguishes between the trajectory intersection with module vertex A (which is glanced with the aircraft continuing to occupy sector s) and the trajectory intersection with a vertical face at B (at which the aircraft leaves sector s and enters sector $s+1$).

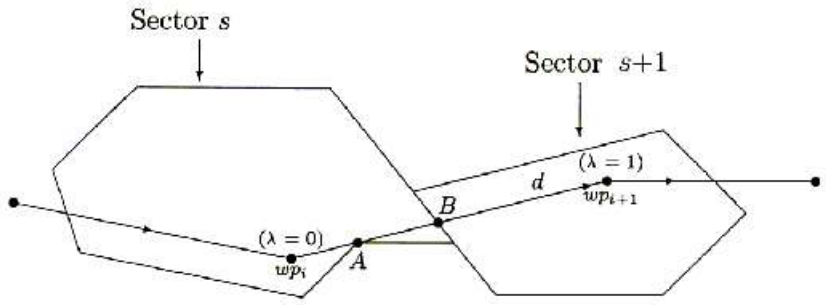

Figure 2-9: Sector Occupancy Calculation Example [48]

2.6.2. Aircraft Encounter Model

Sherali et al. [48] have also developed the Aircraft Encounter Model (AEM). This model is deterministic with respect to aircraft position. The model accepts as inputs a set of flight plans, each expressed as a series of waypoint information in 4-dimensional

space $(x_1, x_2, x_3, \text{time})$, and the sector occupancy information produced by the AOM model.

A conflict occurs when any intruder aircraft passes within the proximity shell constructed around a focal aircraft as depicted in Figure 2-10. To examine possible intruder conflicts with the focal aircraft, a transformation matrix Q is used to convert Cartesian coordinates of the aircraft pair into a system that is aligned with the focal aircraft's positive in-trail axis, denoted d^A. This transformation is described in more detail in Chapter 3. Note that a different Q transformation must be used for each piecewise linear trajectory segment of the focal aircraft.

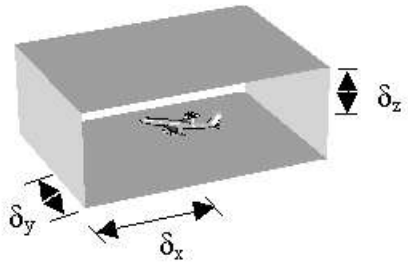

Figure 2-10: Aircraft Separation Box

Figure 2-11 depicts a conflict (in two dimensions). Note that when aircraft B conflicts with aircraft A, the reverse is not necessarily implied. Hence the AEM algorithm looks for potential conflicts between aircraft pairs with each aircraft treated alternatively as the focal aircraft.

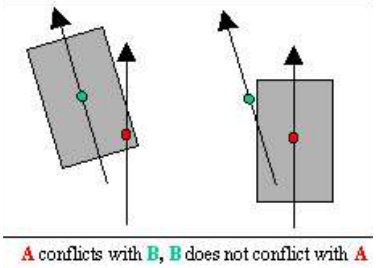

Figure 2-11: Aircraft Conflict

During a scaled time interval $0 \le \lambda \le 1$ (where time has also been shifted to the origin), the aircraft A traverses the linear trajectory between some adjacent waypoints. As shown in Sherali et al. [48], aircraft B conflicts with A when (2.9) is satisfied. This relation decomposes to six inequalities, with two in each spatial dimension.

$$-\delta \le Q^t\left(\overline{x}^B - \overline{x}^A\right) + \lambda \cdot Q^t(d^B - d^A) \le \delta\,. \tag{2.9}$$

This calculation is repeated for all potential intruder aircraft as the focal aircraft moves along its trajectory between successive pairs of adjacent waypoints. The model generates time intervals for which conflicts with different intruder aircraft are identified. Figure 2-12 provides an example of a conflict Gantt Chart created for a single focal aircraft.

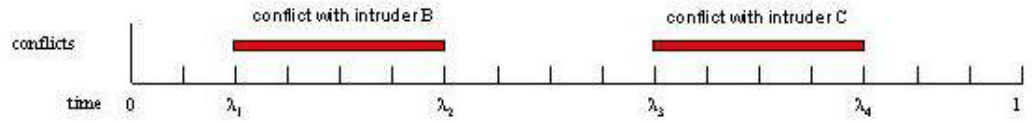

Figure 2-12: Conflict Gantt Chart for Aircraft A Between Two Waypoints

The AEM model outputs these deterministic conflicts to an Airspace Planning Model (APM) that is described next, where they are used to create the conflict constraint set.

2.6.3. Preliminary Airspace Planning Model (APM)

The APM of Sherali et al. [47] selects optimal flight plans from among a set of alternative flight plans called surrogates. The model addresses safety, workload, and equity concerns. It examines collision risk (using the outputs of AOM and AEM) between flights and eliminates conflicting flight pairs that exceed the ability of Air Traffic Controllers to safely redirect. Next, the model constrains traffic flow through sectors of the NAS based on their respective capacities. In addition, APM makes provisions for temporary reductions in sector capacity, such as those caused by weather conditions or

though the creation of SUAs. Finally, the model seeks a solution that does not unfairly burden participating airlines by equitably distributing the delay and fuel costs arising from the collective solution that trades off between the conflicting priorities of the various airlines.

A brief overview of the formulation and notation of the APM [47] is given below.

Model APM:

Minimize: $$\sum_{f=1}^{F}\sum_{p\in P_f} c_{fp}x_{fp} + \sum_{s\in S}\sum_{n_s=1}^{\bar{n}_s} \mu_{sn}y_{sn} + \mu_e\left(x_u^e - x_l^e\right) + \mu_u^e x_u^e \,. \quad (2.10a)$$

Subject To: $$\sum_{p\in P_f} x_{fp} = 1 \quad \forall f = 1,...,F \quad (2.10b)$$

$$\sum_{(f,p)\in C_{si}} x_{fp} - n_s \le 0 \quad \forall i = 1,...,M_s, \forall s \quad (2.10c)$$

$$n_s = \sum_{n=1}^{\bar{n}_s} n\, y_{sn} \quad \forall s \in S \quad (2.10d)$$

$$\sum_{n=1}^{\bar{n}_s} y_{sn} = 1 \quad \forall s \in S \quad (2.10e)$$

$$x_l^e \le U_\alpha(x) \le x_u^e \quad \forall \alpha = 1,...,\bar{\alpha} \quad (2.10f)$$

$$x_P + x_Q \le 1 \quad \forall (P,Q) \in FC \quad (2.10g)$$

$$\sum_{P\in S_k} x_P \le |S_k| - 1 \quad \forall k \in K_{NR} \quad (2.10h)$$

$$x \text{ binary}, y \ge 0, x_l^e \ge 0, x_u^e \le \nu_e \quad (2.10i)$$

There are F flights being considered with one flight plan p to be selected from among the $p \in P_f$ surrogates for each $f = 1,...,F$. The binary decision variable x_{fp} equals one if flight plan $p \in P_f$ is selected for flight f, and zero otherwise, and has the cost c_{fp} associated with it.

The second term in (2.10a) addresses sector workloads and is formulated as a penalty function. At most $\bar{n}_s$ flights can simultaneously occupy the sector s (belonging to the set of S sectors being examined) including flights occupying adjacent sectors that

are in conflict with flights in s. The binary variable y_{sn} equals one when there is a maximum of n_s flights in s during a specified time horizon and μ_{sn} is the corresponding assigned penalty.

The last two terms of the objective function consider equity. The "utility-based measure of effectiveness" is defined in the APM as

$$U_\alpha(x) \equiv \sum_{(f,p)\in A_\alpha} u_{fp} x_{fp} \,, \tag{2.11}$$

where u_{fp} is the excess cost incurred by airline α (from the set of $\bar{\alpha}$ participating airlines) when flight plan p is selected for flight f. This excess cost is the expense incurred by the airline that is in addition to the cost had the airline been able to select the minimal cost flight plan (based on the airline's own prioritization scheme). The penalty μ_e is assigned for the variation in these excess costs, ($x_u^e - x_l^e$), where $x_l^e \geq 0$ and $x_u^e \leq \nu_e$, for some limiting tolerance ν_e. The effect of this penalty is to minimize the spread (i.e. inequity) of costs associated with the collaborative decision made between the airlines. Finally, the penalty μ_u^e is assigned for the maximum measure of excess cost incurred.

The APM includes three types of restrictions on the selection of flight plans via the constraint formulation. First, decision equity is considered. The measure of effectiveness, defined in (2.11), is bounded between a minimum and maximum, and is given by (2.10f) and (2.10i).

Next, the air traffic management workload for each of the sectors is considered. Sector workload is defined as the number of aircraft present in that sector's airspace region as a function of time. Recall that sector occupancy information is provided by the AOM output. The variable n_s is defined as the maximum number of flights simultaneously occupying sector s, and is bounded on the interval $[1, \bar{n}_s]$. The APM determines the value of n_s by examining maximal overlapping sets of conflicts occurring in sector s throughout the time horizon, using an algorithm developed by Sherali and

Brown [45]. We discuss this aspect of workload constraint formulation in more detail in Chapter 4. For sector s, $i = 1,...,M_s$ indexes the collection of maximal overlapping sets and

$$C_{si} = \left\{(f,p) : (f,p) \in i^{\text{th}} \text{ maximal overlapping set for sector } s\right\}, \forall i = 1,...,M_s, \forall s \text{ .} \quad (2.12)$$

The penalty function μ_{sn} is assumed to be increasing nonlinearly for increasing n_s. Accordingly, the constraints (2.10c-e) are included in the APM.

Sherali et al. [47] show that the binary restrictions on y_{sn} hold automatically at optimality along with the integer and bounding restrictions on $n_s, \forall s$. Hence, the continuous relaxation for these variables are used in the formulation.

Finally, the APM considers conflict resolution restrictions. The model prohibits fatal conflicts via (2.10g), defined as when an aircraft penetrates the inviolable airspace surrounding another aircraft. Non-fatal conflicts are restricted by (2.10h) to be no more than a specified maximum number occurring in sector s during any time interval t. The methodology for restricting non-fatal conflicts is discussed in detail in Chapter 3.

2.6.4. Proposed Airspace Planning and Collaborative Decision Making Model (APCDM)

The APCDM proposed herein builds upon the foundation made by the preliminary APM. This model will utilize an inner-outer iterative structure. Figure 2-13 depicts the APCDM structure.

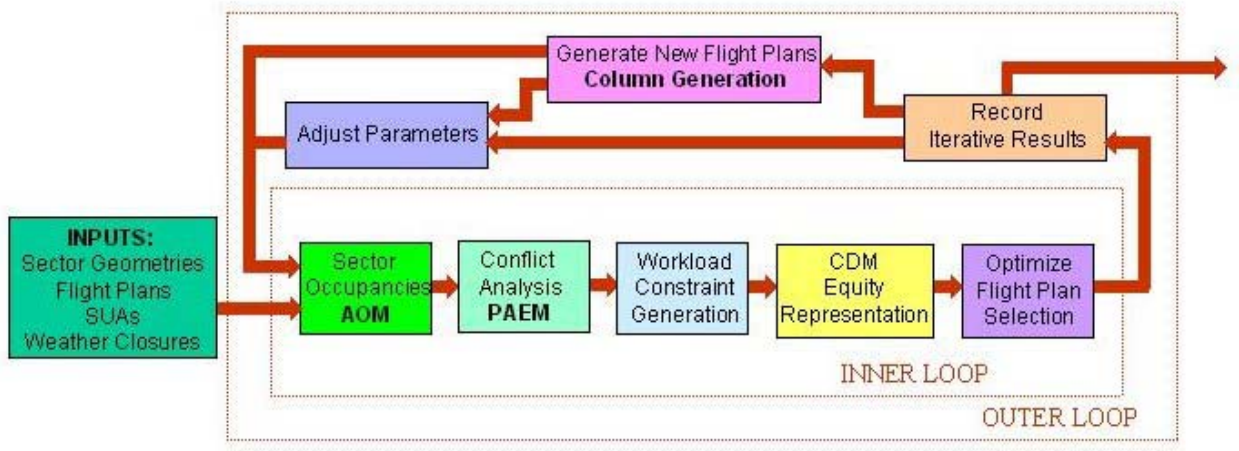

Figure 2-13: APCDM Structure

The inputs to the APCDM are the set of proposed flight plans (including a number of alterative surrogate plans corresponding to each flight) and the sector geometries. We shall also consider reductions in sector capacities due to SUAs and weather-related closures. In addition to the deterministic analysis previously performed in APM, we shall examine stochastic time-dependant restrictions that may ultimately prohibit the selection of some subset of these flight plan alternatives.

The inner loop begins with the AOM model (which is used without significant change from [48]). The Probabilistic Aircraft Encounter Model (PAEM), introduced in Chapter 3, is the next module of the inner loop, where we employ a stochastic approach with respect to aircraft position (versus the deterministic approach of the AEM model) to better reflect the uncertainties with respect to flight plan execution. We shall experiment with several probability distributions and conflict probability thresholds to examine their respective influence on the overall APCDM model and its results.

We use the PAEM output (in a similar manner as AEM was used) to provide the necessary information for developing the sector workload constraints. We shall experiment with several classes of valid inequalities (discussed in Chapter 4) for the constraint set in an effort to improve the solvability of larger models.

In Chapter 5 we will discuss the next module that addresses equity considerations for selecting flight plans, using a utility-based approach. We will look at several factors that may influence participant decisions in a CDM environment.

The final module of the APCDM inner loop is the mixed-integer optimization model itself. We will use CPLEX-MIP 7.0 [12] to solve the enhanced model representation.

In the outer loop, we shall examine the results of the optimization model, and explore a strategy for generating new flight plans via column generation techniques, as well as possibly modify suitable model parameters. These new surrogates will be generated from the viewpoint of time-dependent SUAs or weather-related airspace closures, direct-to routings, conflict avoidance, and equitable cost distributions.